Oligothiophene Bipyridine Alternate Copolymers and Their Ruthenium Metalated Analogues: In Situ ESR and UV−Vis Investigations of Metal−Chain Interactions

F. Lafolet,[†] F. Genoud,[‡] B. Divisia-Blohorn,*[,†] C. Aronica,[†] and S. Guillerez[†]

Groupe d'Electronique Moléculaire and Laboratoire de Physique des Métaux Synthétiques, Unité Mixte de Recherche CEA−CNRS−Université-J. Fourier No. 5819, CEA-Grenoble, 17 rue des Martyrs, 38054 Grenoble Cedex 09, France

Received: April 8, 2005; In Final Form: May 2, 2005

In situ electron spin resonance (ESR) and UV−vis spectro-electrochemical studies have been performed on two copolymers consisting of alternating subunits of regioregular head to tail (HT) coupled 3-octylthiophene tetramer and 2,2′-bipyridine subunits (**P4)** or 3-octylthiophene hexamer subunits of the same regioregularity and 2,2′-bipyridine subunits (**P6**). Both **P4** and **P6** have been investigated in their metal-free form as well as in the ruthenium(II) metalated form (**P4−Ru** and **P6−Ru**). **P4** and **P6** in the p-doped state exhibit a clear ESR signal characteristic of the presence of polarons in the oligothienylene subunits. In the case of **P4**, no recombination of polarons into bipolarons is observed, whereas the recombination process takes place in **P6**. The formation of bipolarons is well-rationalized in terms of the conjugation length, and it seems clear that the higher length of the oligothiophene subunit in **P6** stabilizes bipolarons. The same effect, is induced by the coordination of $-Ru(bpy)_2^{2+}$ to the bipyridine unit in the metalated form of both polymers, which results in an increase of the conjugation length. Important information is gained from the analysis of the ESR spectra of both nonmetalated and metalated in the oxidized (p-doped) and reduced (n-doped) forms. In the p-doped state both nonmetalated and metalated polymers reveal the presence of a narrow ESR line characteristic of the mobile spin carriers in the polymer matrix. The oxidation of the metal center occurs at higher potentials and leads to an irreversible destruction of the system. To the contrary, in the reduced (n-doped) state the ESR lines of the nonmetalated and metalated polymers markedly differ. A significant line broadening with simultaneous change of the *g*-value is caused by spin−orbit coupling phenomenon induced by the presence of the coordinating metal. Finally, the observation of a clear polaronic band in the UV−vis spectrum of p-doped **P4** and its strong dependence on the applied potential can be clearly correlated with the potential induced changes in the ESR spin density. The same applies to **P4−Ru**, where the changes in the polaronic and bipolaronic bands can also be correlated with the ESR spin density changes.

Introduction

Conjugated metallopolymers are an important novel class of materials whose unusual properties originate from the coupling of the chemical, electronic, and optical properties of the conjugated backbone to those of the metal center. The interest of such materials is stimulated by their numerous promising applications in electronic or optoelectronic devices, such as plastic thin film transistors and sensors etc., which have recently been reported in several reviews.[1] Two challenges confront researchers developing these materials: first, the synthesis of suitable metal-containing monomers, their polymerization in a controlled manner, and the processing ability of synthesized polymers; second, the development of an understanding of the nature and the extent of the electronic coupling between the metal and the conjugated polymer backbone.

In our synthetic approach, we have developed two strategies. In the first one, electropolymerization of specifically designed monomers using the powerful templating effect of a series of first-row transition metals (mostly Cu(I)) is used which leads to a set of conjugated, catenane-like metallopolymers or conjugated polymetallorotaxanes. In these materials, the coordination site is constituted by rigid phenanthroline units. Consequently the metallopolymers exhibit various interesting topographical and topological properties.[2] In the second approach, soluble and easily processible conjugated metallopolymers incorporating heavy metals such as ruthenium or osmium are prepared. They consist of different regioregular (3-alkyl)thiophene oligomers alternating with metal chelating 2,2′-bipyridine units of low rigidity.[3,4] The regioregular distribution pattern of the alkyl groups improves electronic delocalization along the oligothienyl moieties as compared to regiostatistical distribution.[5] However, depending on the position of the alkyl substituents in the oligothienyl−bipyridyl linkages with respect to the bipyridine subunit, different steric phenomena can be induced. In particular, statistically one of the two oligothienylene−bipyridine linkages should be twisted due to the steric constraints. This leads in turn to a reduced electronic communication between the metallic complex and the oligothiophene.[6]

For both types of polymers, the metal affects the polymer backbone properties via its redox state and a combination of steric and inductive effects. The characterization of the electronic interactions between two adjacent metals or between the metal centers and the oligothienyl moieties requires the use of spectro-

* Corresponding author. Phone: 33-43878-84450. Fax: 33-43878-5145. E-mail: bblohorn@cea.fr.
[†] Group d'Electronique Moléculaire.
[‡] Laboratoire de Physique des Métaux Synthétiques.

10.1021/jp051824b CCC: $30.25
Published on Web 06/14/2005

CHART 1: General Formula of Polymers P4 and P6 and Their Analogous Ruthenated Polymers P4−Ru and P6−Ru

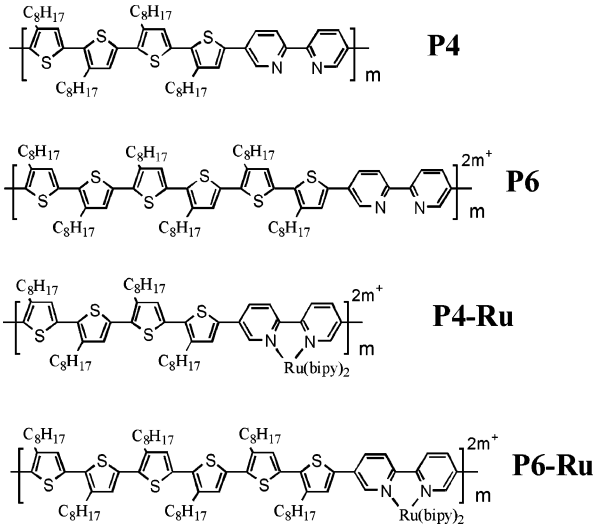

electrochemical methods in which the spectral response is coupled to the electrochemical one. For example, steric constraints around the copper center in catenane-like metallopolymers[7] and polymetallorotaxanes[8] have been observed by X-ray spectroscopy absorption (EXAFS), while the nature of charge carriers,[9] i.e., the polaron and bipolaron of oligothienyl moieties and the paramagnetic metal center Cu(II), have been successfully studied by the electron spin resonance (ESR) spectro-electrochemistry. Recently, the communication between the metal centers and the π-conjugated backbone of polythiophene−bipyridyls containing Ru(II) has been demonstrated by subtractively normalized interfacial Fourier transform infrared spectroscopy (SNIFTIRS) coupled to electrochemistry investigations. The results show that the metal centers function as "electronic gates", allowing charge to be inserted into the polymer at reduced potentials.[10]

To better elucidate the nature of the redox processes occurring in these conjugated metallopolymers as well as in their metal-free analogues, we have carried out a comparative investigation of their electrochemical behavior combined with in situ ESR and UV−visible spectroscopies. The goal of these investigations is to correlate the redox states and the nature of charge storage configurations in the p- and n-doped polymers and to verify whether the existing polaron−bipolaron model can explain the observed phenomena.[11] We focus on two copolymers consisting of alternating subunits of regioregular head to tail (HT) coupled 3-octylthiophene oligomers and 2,2′-bipyridine subunits. The investigated polymers in their nonmetalated and in the Ru metalated forms are depicted in Chart 1, together with their abbreviations.

Experimental Section

Reagents, Electrochemical, and Spectroelectrochemical Procedures. The preparation of **P4** and **P4-Ru**[3] and **P6 and P6-Ru**[4] has been described previously. The molecular weights of the polymers studied in this research were as follows: **P4**, M_n = 111 000, PI = 2.2 (GPC, polystyrene standards); **P4−Ru**, M_n = 29 000 (NMR), M_w = 70 000 (light scattering), PI = 2.4; **P6**, M_n = 56 000, PI = 1.9 (GPC, polystyrene standards); **P6−Ru**, M_n = 27 000 (NMR), M_w = 70 000 (light scattering), PI = 2.6.

All experiments were carried out under an anhydrous, oxygen-free argon atmosphere. Acetonitrile (CH_3CN) and chloroform ($CHCl_3$) purchased from SDS chemical supplier (99.9%) were distilled over sodium hydride or P_2O_5 and stored in a drybox in argon atmosphere. The supporting electrolytes n-Bu_4NPF_6 and n-Bu_4NClO_4 were purchased from Fluka (puriss. p.a.) and used as received.

Fresh films were prepared prior to experiments. For UV−vis and ESR spectro-electrochemical investigations, the polymers were deposited by spin coating from 0.6 mL of 3 g L^{-1} solutions on an ITO (indium−tin oxide) transparent electrode or by dip coating onto a platinum wire electrode, respectively. **P4** and **P6** were dissolved in $CHCl_3$, and **P4−Ru** and **P6−Ru** were dissolved in CH_3CN. The cyclic voltammetry (CV) measurements were carried out in a one-compartment cell with a platinum counter electrode and an Ag wire electrode as pseudoreference. The pseudoreference electrode was checked against the ferrocene/ferricinium couple ($E_{1/2}(Fc^+/Fc)$ = 0.14 V/Ag) after each experiment, when possible. The electrolyte solutions were 0.1 M n-Bu_4NPF_6 in CH_3CN in the investigations of **P4** and **P6** and 0.4 M n-Bu_4NClO_4 in CH_3CN in the case of the studies of **P4−Ru** and **P6−Ru**.

UV−Vis Spectro-electrochemistry. UV−vis spectro-electrochemical experiments were carried out with a diode array UV−visible spectrometer Spectra-Pro 150 (Acton Research Corp.) and a PGZ 301 potentiostat (Voltalab, France). A thin layer of the polymer was deposited in a transparent ITO electrode and placed into a small quartz spectro-electrochemical cell equipped with a platinum wire counter electrode and an Ag wire pseudoreference electrode. The voltage was applied over the anodic potential window from 0 to 1.6 V vs Ag. The in situ UV−vis spectro-electrochemical measurements were synchronized by a monitoring system Sync 200 (Radiometer Analytical, France). The detector was a CCD RTEA/CCD-128-H camera controlled by a chopper ST 133 (Princeton Instruments, Inc.). The light source was a XS 432 60 W (Eurosep) lamp with an optical fiber LG-455-020-1 (Princeton Instruments) and an Acton Small shutter. The potential scan rate was 20 mV s^{-1} coupled to the spectrometer to record one UV−vis spectrum per second.

ESR Spectro-electrochemistry. ESR spectro-electrochemical experiments were carried out with an ER 200 X band Brüker spectrometer in a small electrochemical quartz cell with two platinum wires (working and counter electrodes) and an Ag pseudoreference electrode. Polymer films were cast onto the working electrode as described previously. After rinsing, the film adhering to the electrode was transferred to the ESR spectro-electrochemical cell containing the same electrolyte as in the case of the cyclic voltammetry and UV−vis spectro-electrochemical studies. The redox state of the polymer was monitored by a DC voltage applied to the working electrode over a cathodic potential window ranging from 0 to −3.5 V vs Ag and an anodic potential window from 0 to 1.5 V vs Ag in small increments of 0.020 V. For each experimental point the ESR susceptibility was determined by double integration of the ESR signal.

Results and Discussion

P4 and **P6** are electroactive**,** their representative cyclic voltammograms being shown in Figure 1. The CV curves of **P4−Ru** and **P6−Ru** are given in Figures S1 and S2, and all electrochemical data are collected in Table 1.

In all metalated and demetalated polymers studied different well-defined redox waves can be found. They correspond to the p-and n-doped states and can be assigned to charge localization on metal centers, π-conjugated polymer backbone,

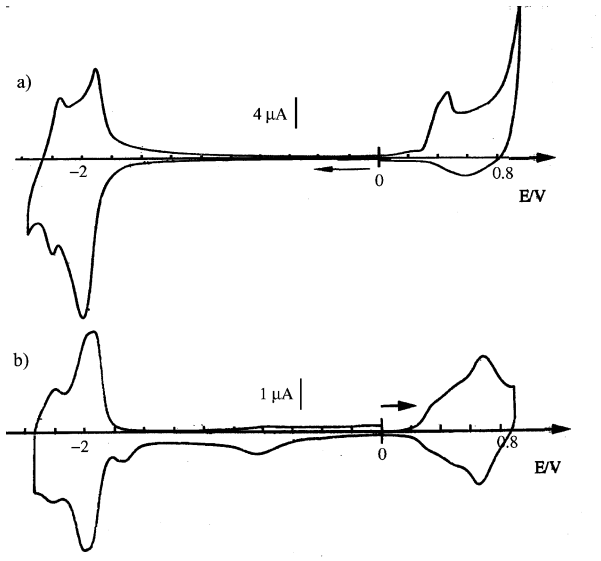

Figure 1. Cyclic voltammetry (10 mV s^{-1}) in tetrahydrofuran (THF) [n-Bu_4N]ClO_4 (0.4 mol L^{-1}), Pt electrode (S = 0.07 cm^2), Ag^+/Ag reference, of freshly prepared films of (a) **P4** and (b) **P6**.

or ancillary bipyridines. The detailed analysis of their voltammetric properties can be found elsewhere,[4] except for **P6** which exhibit similar electrochemical behavior as **P4**. Here we limit ourselves to the ESR and UV−vis spectro-electrochemical response.

In Situ ESR−CV Spectro-electrochemical Studies. Since ESR is extremely sensitive to the presence of even minute amounts of paramagnetic species, it is very risky to interpret the obtained ESR response without verifying the background spectra, i.e., the spectra obtained without a thin film of the polymer deposited on the electrode. The ESR investigation of the electrolyte gave an extremely weak, essentially non-measurable ESR signal. We present this spectrum in Figure S3.

In the case of the metalated forms of the polymers studied (**P4−Ru** and **P6−Ru)** the oxidation of Ru(II) into Ru(III) in the potential range corresponding to the third oxidation wave of CVs should give a characteristic ESR signal of Ru(III) species.[12] All attempts to observe ESR signals of paramagnetic Ru(III) were unsuccessful, which is in contrast with the case of copper polymetallorotaxanes,[9] where one signal attributed to the copper(II) ion was observed during the oxidation of the polymer. In the case of ruthenated polymers, the absence of an ESR signal ascribed to Ru(III) species can be explained by their low stability at the metal oxidation potential, due to the overoxidation of the matrix mediated by Ru(III). For both metalated and nonmetalated polymers studied, only an unresolved single line, characteristic of organic species, has been observed for both the anodic and the cathodic electrochemical scans. Representative ESR spectra are presented in Figure 2; their corresponding peak to peak line width ΔH_{p-p} and g factors are collected in Table 2.

p-Doped Polymer Investigations. All ESR lines, associated with the p-doped states of the metal free and the ruthenated polymers, are centered roughly at the same magnetic field (Figure 2). Moreover, the g-factors values ($2.0020 < g < 2.0032$) are close to the free electron value and in the range reported for various conducting polymers.[13] Evidently the spins originate from the presence of radical cations (polarons) in the polymer backbone (Pn−$bpy^{\bullet+}$, n = 4, 6).[14] The appearance of a rather sharp Lorentzian signal indicates the formation of mobile polarons in all studied polymers (even in the metalated ones), consistent with the charge carrier transport occurring along the carbon skeleton of the polymeric backbone.[15] The line width of the ESR signal in polyconjugated systems can be taken as a measure of the charge carriers mobility. As judged from the ΔH_{p-p} values ($1.7\ G < \Delta H_{p-p} < 3.0\ G$), the mobility of polarons in the oligothiophene−bipyridine alternate copolymers studied here is lower than that measured for oligooctylthiophene films ($\Delta H_{p-p} = 1.3$ G).[16] The absence of any significant effect of the thiophene oligomer subunit length on the line width and a hardly measurable influence of the presence of the coordinated metal on the ESR line parameters seem to indicate that the hole transport is only moderately affected by structural modifications of the conjugated backbone. It is worth noting that our previous measurements of the field effect mobility in the same polymers, which have clearly shown that the transport phenomena are governed by the polymer structure.[17] This apparent discrepancy highlights the scales of explored phenomena. For the field effect transistor measurements, the 3-D structure of the materials, i.e., the packing of conjugated chains, plays the major role and is deeply affected by the grafting of the bulky substituents such as the ruthenium bis(2,2′-bipyridine) moiety. To the contrary, the ESR measurements seem to be insensitive to this long-range order and rather probe the intrachain transport processes.

Figure 3 shows the dependence of the ESR magnetic susceptibility vs potential registered in the anodic potential range for the ruthenated and the nonmetalated polymers. In the case of ruthenated polymers, the anodic scan was limited to the potential range corresponding to the backbone oxidation in order to avoid any overoxidation of the conjugated oligomer segments originating from the formation of the strongly oxidizing Ru(III) species. With the exception of **P4**, which exhibits residual spins, the ESR signal appears only when the applied potential reaches the onset of the wave corresponding to the oxidation of the polymer backbone. Two different behaviors have been observed during the p-doping of these polymers. On one hand, the evolution of the magnetic susceptibility for **P6**, **P4−Ru**, and **P6−Ru** clearly indicates that the electron spin density reaches a maximum at the potential corresponding to the first one-electron oxidation process. This process can be attributed to the formation of radical cations (Pn−$bpy^{\bullet+}$, n = 4, 6) due to the oxidation of polymer backbone. When the potential is raised to more anodic values, the spin population decreases as a result of the recombination of spins located on adjacent sites. Upon the backward scan, the reverse process, i.e., the dissociation of bipolarons into polarons, is observed with some cathodic shift. This indicates that the spin recombination process is reversible and can be electrochemically controlled. The incomplete decrease of the spin density of **P6** and **P4−Ru** upon the backward scan is probably associated with their chemical instability under experimental conditions. The presence of a clear maximum in the anodic scan of **P6**, **P4−Ru**, and **P6−Ru** seems to suggest that the doping can be discussed in terms of the classical polaron−bipolaron model, which well-correlates with their electrochemical properties.

In the case of **P4**, two successive forward and backward potential scans were performed (Figure 3). Upon scanning over the potential range limited to the first two oxidation waves, the ESR susceptibility increases regularly without showing any maximum, which would be expected in the case of the polaron recombination. Similar monotonic decrease is observed in the reverse. When the polymer oxidized to higher potentials, a maximum of the susceptibility can be reached. However the continuous decrease of the spin population upon the backward scan indicates that this maximum may not be associated with

TABLE 1: Half-Wave Potential Values $E_{1/2}$ of Polymers[a]

	p-doped states[b]			n-doped states[b]		
	$E(1)_{1/2}$ (V)	$E(2)_{1/2}$ (V)	$E(3)_{1/2}$ (V)	$E(4)_{1/2}$ (V)	$E(5)_{1/2}$ (V)	$E(6)_{1/2}$ (V)
P4	0.68	1.06		−2.07[c]		−2.2
P6	0.68	0.86		−2.07[c]		−2.2
P4−Ru	0.68	0.84	1.11	−1.28	−1.56	d
P6−Ru	0.53	0.69	1.05	−1.28	−1.59	d

[a] $E_{1/2}$ defined as $^1/_2(E_{pa} + E_{pc})$ vs pseudo Ag^+/Ag reference used in ESR experiments. [b] (1) and (2) refer to processes localized on the conjugated backbone, (3) on the metal, (4) and (6) on bpy linked to oligothienyls, (5) on ancillary bpy. [c] Two-electron transfer. [d] Not well-defined wave: E_{pc} approximately equal to −2.5 V.

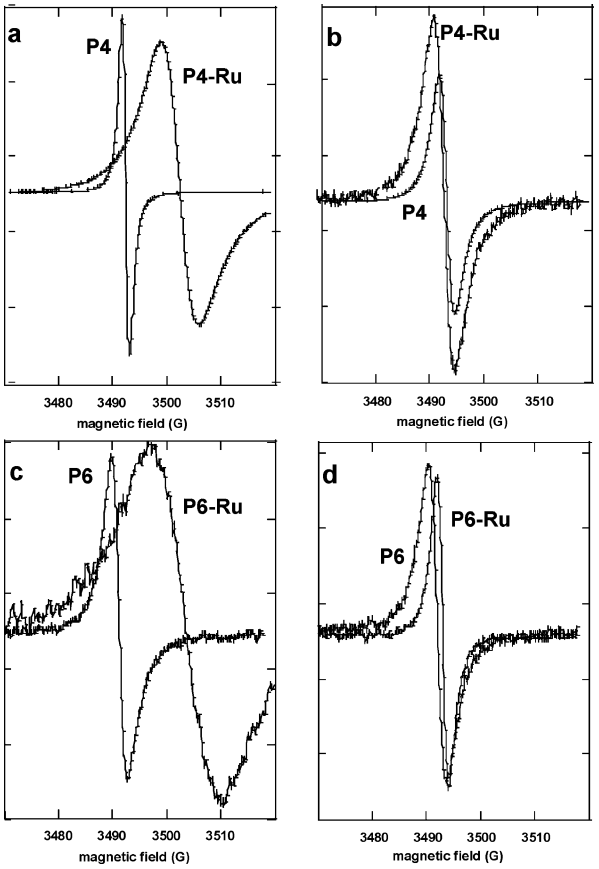

Figure 2. Representative ESR spectra (arbitrary unity): (top) **P4** and **P4−Ru** (a) in reduced state and (b) in oxidized state; (bottom) **P6** and **P6−Ru** (c) in reduced state and (d) in oxidized state.

TABLE 2: ΔH_{p-p} and *g*-Factors of ESR Spectra Registered on Polymers P4 and P6 and Ruthenated Analogous P4−Ru and P6−Ru in Their p- and n-Doping States

	p-doped states		n-doped states	
	ΔH_{p-p}[a] (G)	g[b]	ΔH_{p-p}[a] (G)	g[b]
P4	1.7	2.0032	1.5	2.0013
P6	2.5	2.0022	2.6	2.0009
P4−Ru	3.0	2.0020	6.9	1.9969
P6−Ru	2.3	2.0026	13	1.9966

[a] Precision: 0.1 G. [b] Precision: 5×10^{-4}.

the recombination of polarons into bipolarons, but more likely originates from an irreversible overoxidation of the polymer. Thus, when the reversible charging of **P4** is considered, only polarons are formed (or alternatively the ratio of polarons to bipolarons must be kept in a constant ratio) and no recombination takes place. This phenomenon is observed only for **P4**, since for **P4−Ru**, **P6**, and **P6−Ru**, the classical mechanism consisting of the successive formation of polarons and bipolarons is experimentally observed. This unusual behavior of **P4** is

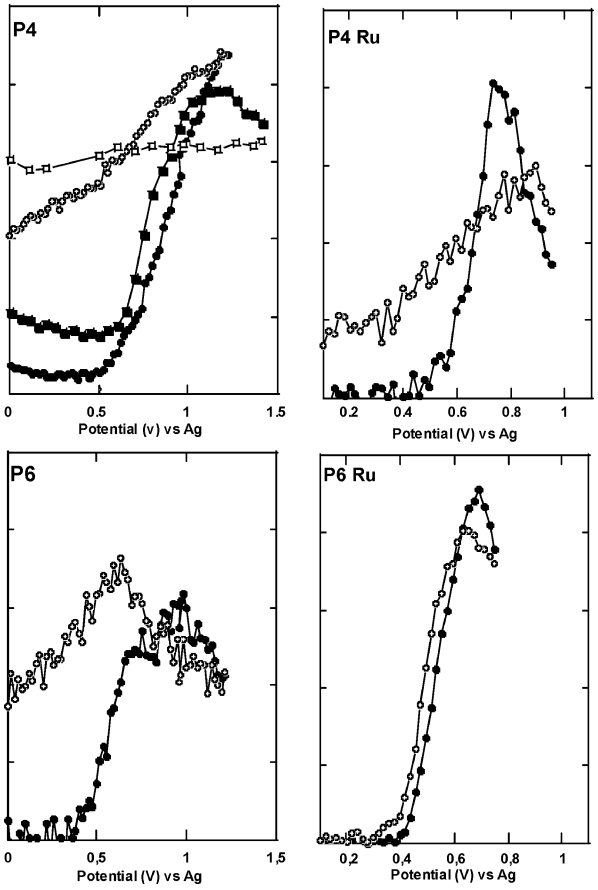

Figure 3. ESR susceptibility vs anodic electrochemical potential on films (arbitrary units; integrated surface area of signal centered at G) during (●) the first oxidation scan, (○) the first reduction scan, (■) the second oxidation scan, and (□) the second reduction scan: (a, top left) **P4**, (b, top right) **P4−Ru**, (c, bottom left) **P6**, and (d, bottom right) **P6−Ru**.

probably associated with its lower conjugation. The thiophene segment is too short to allow the stabilization of two positive charges under our experimental conditions and favors the formation of radical cations. Moreover, the fact that the formation of polarons extends over the potentials of the two successive oxidation waves, clearly seen in the cyclic voltammogram, seems to indicate that tetrathienyl moieties are only weakly electronically coupled through the bipyridyl units. In addition, the charging of the first half of the tetrathienyl units makes the formation of polarons on the remaining neutral sites more difficult. As a result this process takes place at slightly more anodic potentials.[9]

A particularly interesting point of the **P4** metalation is that the complexation of ruthenium(II) induces an extended conjugation length in the alternate copolymer due to the flattening of the bipyridine subunit linked to the conjugated oligothiophene, allowing the stabilization of one dication per repeating unit.

At the end, it should be noted that the reverse potential scan produces a slow decrease of the ESR signal for all polymers except of the case of **P6**−**Ru.** A possible explanation involves the formation of partially soluble fragments of the polymer less accessible to the electroreduction as suggested by a light coloration of the electrolyte at the end of experiment.

n-Doped Polymer Investigations. We have first investigated the reduction (n-doping) of the nonmetalated polymers, i.e., **P4** and **P6**. From the data reported in Table 2, it can be concluded that the *g*-values for the n-doped states are lower than those measured for the p-doped ones (**P4**, $\Delta g = -0.0019$; **P6**, $\Delta g = -0.0013$). This may originate from a different localization of the p- and the n-polarons in the conjugated chain. Indeed, it has been already reported that spin−orbit coupling related to the presence of heavy atoms such as sulfur causes an increase of the *g*-factor.[18,19] For our polymers, the lower values for the *g*-factor observed for the n-polarons is then consistent with a localization of the charge carriers on the bipyridine subunits rather than on the oligothiophene segments. However the similar values of ΔH_{p-p} indicates that, despite their different localizations, the p- and n-polarons have similar mobilities.

Both nonmetalated polymers **P4** and **P6** display, in the cathodic potential range, two unresolved waves at $E_{1/2} = -2.07$ and −2.2 V, respectively. These are assigned to bi- and monoelectronic doping processes, respectively. In the ESR response to the potential change no ESR signal is recorded until $E = -2.2$V for **P4** and $E = -2.5$V for **P6**. At more cathodic potentials a sharp signal appears (vide supra) followed by its vanishing because of the recombination of polarons into bipolarons. These signals appear at very low potentials, especially in the case of **P6**. The origin of this strong overpotential is not well-understood and does not correspond to the first reduction process of the polymers. Since the ESR signal appears in the potential range of the solvent reduction, the verification of the spin response of the electrolyte must additionally be carried out, to avoid a false interpretation. A careful in situ ESR study has been performed on a bare electrode in the electrolyte free of the polymer. No signal was observed under these conditions. Consequently, the results of the in situ ESR experiments carried out for **P4** and **P6** are consistent with the formation of bipolarons, corresponding to the first two-electron reduction process followed by a one-electron reduction process occurring at even more negative potentials (Table 1). Favored bipolaron formation has previously been observed by Yamamoto et al.[20,21] in the n-doping of polypyridines. The reverse scan shows both the electrochemical dependence of the ESR signal shape and position and an hysteresis phenomenon which indicates an important reorganization of the film structure.

The insertion of ruthenium centers into the conjugated polymers has dramatic effects on their behavior in the reduced state. The first reduction processes are shifted toward less negative potentials by about 800 mV and can be assigned to the reduction of the bipyridine segment of the conjugated backbone. Figure 4 shows the evolution of the ESR magnetic susceptibility upon scanning toward negative potentials. For both **P4**−**Ru** and **P6**−**Ru**, a peak of the susceptibility is observed around −1.3 V which corresponds to the two consecutive processes: the creation of the paramagnetic species followed by their immediate annihilation. The peak maximum corresponds to the potential where half of the total charge in the first reduction process is injected. This may be attributed to a stepwise process, consisting, in its first step, of the creation of polarons on the half of the bipyridine units present in the polymer chain. The reduction of the remaining bipyridine units

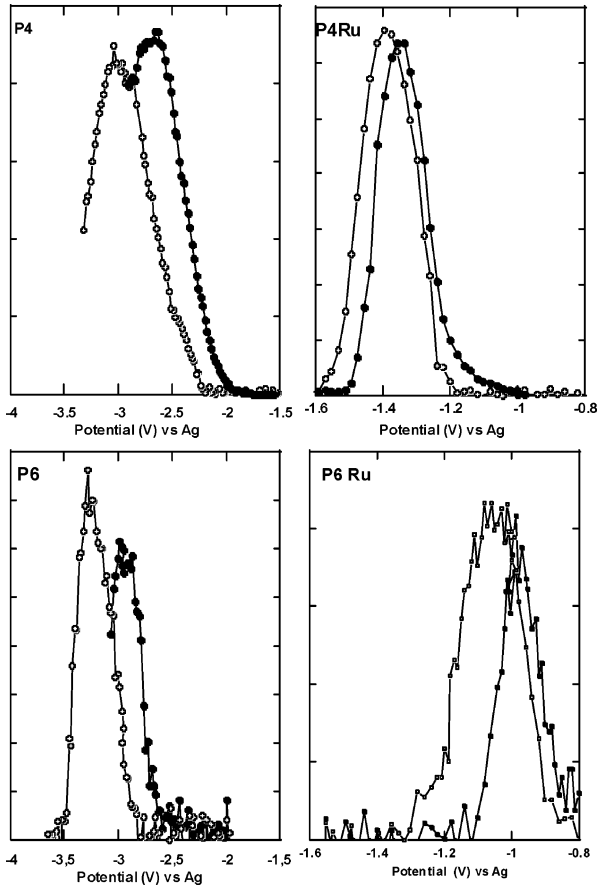

Figure 4. ESR susceptibility versus cathodic electrochemical potential on films (arbitrary units; integrated surface area of signal centered at G) during (●) the first oxidation scan and (○) the first reduction scan: (a, top left) **P4**, (b, top right) **P4**−**Ru**, (c, bottom left) **P6**, and (d, bottom right) **P6**−**Ru**.

leads to the formation of bipolarons because of the electronic coupling between the bipyridine sites through the oligothienyl moiety. This interpretation is supported by our recent finding that the first negative charge injected into ruthenated polymers is partially delocalized over the oligothienyl chains.[10] However, the extent of delocalization remains lower for metalated polymers, as indicated by larger values the peak to peak width found for **P4**−**Ru** and **P6**−**Ru** as compared to the nonmetalated polymers. The lower values of the *g*-factors are in agreement with the previous studies on the reduction of monomeric $[RuL_3]^{2+}$ type complexes[22] and may originate from reduced spin−orbit coupling with ruthenium atoms. This supports the hypothesis of higher localization of n-polarons on bipyridine units for metalated polymers. No ESR signal could be detected at the potentials below −1.6 V, whereas two reduction processes are observed in the CV, suggesting that only polarons are formed.

In Situ UV−**Vis**−**CV Spectro-electrochemical Studies.** Electronic absorption spectroscopy is a very useful tool for the characterization of new electronic states, such as polarons and bipolarons created by the doping of conjugated polymers. The present study on **P4**, **P6**, and **P4**−**Ru** aims to elucidate the role played by (1) the extension of the oligothiophene subunit and (2) the insertion of the ruthenium centers on their electronic properties. The main point is to corroborate the ESR spectroscopy results indicating that **P4** forms polarons upon p-doping, whereas in **P6** and **P4**−**Ru**, the successive formation of polarons and bipolarons is observed. It must be noticed first that **POT**

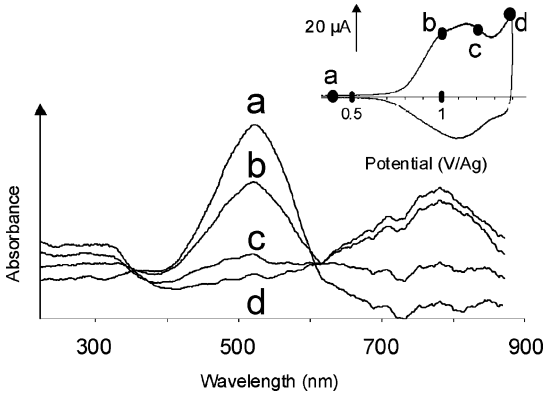

Figure 5. UV−vis spectro-electrochemistry performed on **P4** film spin-coated on ITO electrode in 0.1 M (n-Bu_4N)PF_6/CH_3CN at $\nu = 20$ mV s^{-1}; spectra registered during cyclic voltammetry (insert) at (a) 200, (b) 800, (c) 1200, and (d) 1400 mV vs Ag pseudoreference electrode.

(regioregular poly(3-octylthiophene), which serves as a reference) and **P6** (Figures S4 and S5) behave similarly. The oxidation process is accompanied by a progressive bleaching of the $\pi-\pi^*$ transition band characteristic of the neutral state and peaked around 500 nm. A new band near 800 nm first grows and then decreases before the complete disappearance of the neutral-state band. This behavior is well-documented and corresponds to the preponderant formation of polarons at low doping levels followed by their recombination into bipolarons at higher doping levels.[23,24] As observed by UV−vis spectroscopy (Figure 5), in the case of **P4** the vanishing of the neutral-state transition is accompanied by the concomitant increase of a well-defined band centered at 780 nm. The presence of an isosbestic point at 615 nm indicates the formation of a unique charge-carrier species. The evolution of the low-energy transition can be correlated with the evolution of the magnetic susceptibility observed upon the anodic scan. Normalized absorbance at 780 nm and the susceptibility evolve identically upon the oxidation of the polymer, as shown in Figure 6. From these observations, we can conclude that only polarons are formed upon the p-doping of **P4**. The oxidation of metalated **P4**−**Ru** leads to more complicated features due to the superposition of MLCT and $\pi-\pi^*$ transitions merging into a single broad band centered at 520 nm (Figure 7). At low doping levels, when the potential is limited to the first two oxidation waves, the band associated with the neutral π-conjugated backbone vanishes and the MLCT transition band centered at 480 nm remains unaffected up to 1.0 V (mark d). This confirms our previous assignment of the redox processes, which were based on the electrochemical data only, and allows for the assignment of the third oxidation wave to the Ru(III)/Ru(II) couple. Thus, the oxidation of the π-conjugated skeleton takes place during the two first waves in the potential range limited to 1.1 V. This oxidation appears clearly as a stepwise process with (1) the formation of a well-defined band at 740 nm assigned to polarons and (2) its bleaching and the simultaneous merging of a new intense transition band located in the near-IR region, which can be assigned to the formation of bipolarons. The latter band cannot be detected in the case of **P4**, demonstrating the difference of the behavior induced by the complexation. The evolution of the intensity of the band at 740 nm is in perfect agreement with the evolution of the magnetic susceptibility upon the doping of **P4**−**Ru**, as shown in Figure 6b. This confirms the mechanism of the successive formation of polarons and bipolarons in this polymer.

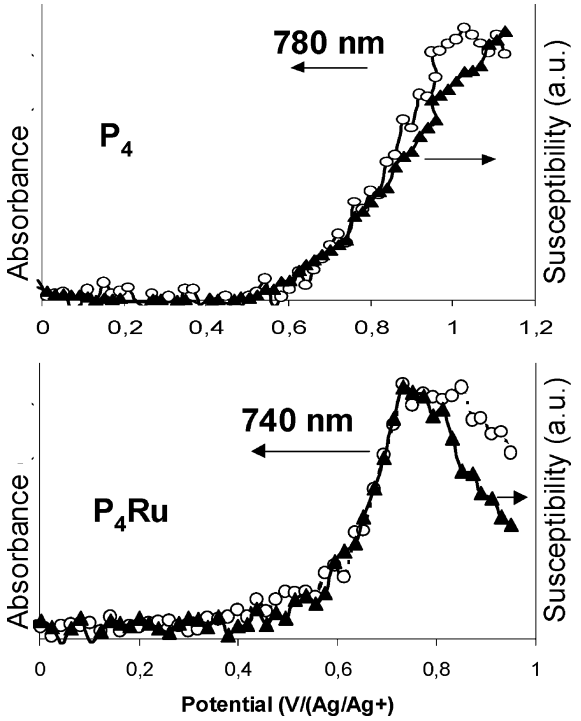

Figure 6. Absorbance at λ and susceptibility in the function of applied potential at $\nu = 20$ mV s^{-1} of films: (a, top) **P4** ($\lambda = 780$ nm) in 0.1 M (n-Bu_4N)PF_6/CH_3CN; (b, bottom) **P4**−**Ru** ($\lambda = 740$ nm) in 0.4 M (n-Bu_4N)ClO_4/CH_3CN.

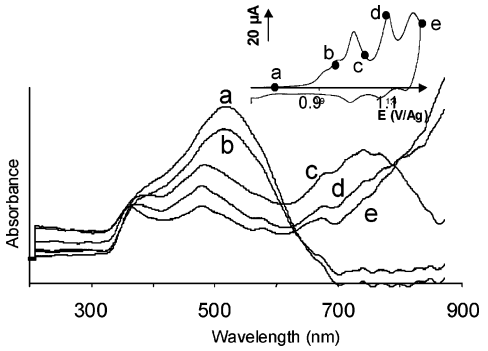

Figure 7. UV−vis spectro-electrochemistry performed on **P4**−**Ru** film spin-coated on ITO electrode in 0.4 M (n-Bu_4N)ClO_4/CH_3CN at $\nu = 20$ mV s^{-1}; spectra registered during cyclic voltammetry (insert) at (a) 600, (b) 1000, (c) 1200, (d) 1400, and (e) 1600 mV vs Ag pseudo-reference electrode.

Conclusion

To summarize, EPR and UV−vis spectro-electrochemical investigations carried out for alternate copolymers consisting of oligoalkylthiphene subunits and bipyridine ones show that, during the p-doping, the polymers studied exhibit the classical sequence of processes involving the formation of polarons followed by their recombination to bipolarons. The only exception is **P4** in which the recombination process is inhibited. This difference is satisfactorily explained in terms of the effective conjugation length in the polymer backbone, caused by the higher length of oligothiophene moieties or by the coordination of $-Ru(bpy)_2^{2+}$ to the bipyridine unit. The last conclusion is well-corroborated by UV−vis spectro-electrochemical experiments. In the case of the n-doping, the ESR signals confirm the localization of polarons on the polymer backbone with their consecutive recombination into bipolarons. In the case of ruthenated polymers, the onset of the ESR signals undergoes an anodic shift. In the same time a narrowing of the

potential window of electrochemical spin response is observed as compared to the case of the nonmetalated analogues. In addition, a strong spin−orbit coupling is observed, indicating that the injection of the charge occurs preferentially on the bipyridine units of the polymer ligand, which act as an electronic gate.

Acknowledgment. The authors acknowledge Dr. Adam Pron (CEA-Grenoble) and Prof. Timothy Hanks (Furman University, South Carolina) for helpful discussions.

Supporting Information Available: Text and figures showing the CV of **P4**−**Ru** and **P6**−**Ru**, the comparison of ESR signal of pure electrolyte and **P6**, and UV−vis spectra of **POT** and **P6** recorded during spectro-electrochemical experiments (PDF). This material is available free of charge via the Internet at http://pubs.acs.org.

References and Notes

(1) (a) Pickup, P. G. *J. Mater. Chem.* **1999**, *9*, 1641. (b) Goldenberg, L. M.; Bryce, M. R.; Petty, M. C. *J. Mater. Chem.* **1999**, *9*, 1957. (c) Kingsborough, R. P.; Swager, T. M. *Prog. Inorg. Chem.* **1999**, *48*, 123. (d) McQuade, D. T.; Pullen, A. E.; Swager, T. M. *Chem. Rev.* **2000,** *100*, 2537. (e) MacLean, B. J.; Pickup, P. G. *J. Mater. Chem.* **2001**, *11*, 1357. (f) Wolf, M. O. *Adv. Chem.* **2001**, *13*, 545. (g) Liu, Y.; Li Y.; Schanze, K. S. *J. Photochem. Photobiol., C* **2002**, *3*, 1. (h) Hirao, T. *Coord. Chem. Rev.* **2002**, *226*, 81. (i) Stott, T. L.; Wolf, M. O. *Coord. Chem. Rev.* **2003**, *246*, 89. (j) Cameron, C. G.; MacLean, B. J.; Pickup, P. G. *Macromol. Symp.* **2003**, *196*, 165.

(2) Kern, J. M.; Sauvage, J. P.; Bidan, G.; Divisia-Blohorn, B. *J. Polym. Sci., Part A: Polym. Chem.* **2003**, *41*, 3470.

(3) Trouillet, L.; De Nicola, A.; Guillerez, S. *Chem. Mater.* **2000**, *12*, 1611.

(4) Walters, K. A.; Trouillet, L.; Guillerez, S.; Schanze, K. S. *Inorg. Chem.* **2000**, *39*, 5496.

(5) (a) McCullough, R. D.; Lowe, R. D. *J. Chem. Soc., Chem. Commun.* **1992**, 70. (b) Chen, T.-A.; Rieke, R. D. *J. Am. Chem. Soc.* **1992**, *114*, 10087. (c) McCullough, R. D.; Lowe, R. D.; Jayaraman, M.; Anderson, D. L. *J. Org. Chem.* **1993**, *58*, 904. (d) McCullough, R. D.; Lowe, R. D.; Jayaraman, M.; Ewbank, P. C.; Anderson, D. L. *Synth. Met.* **1993**, *55*, 1198. (e) McCullough, R. D.; Tristam-Nagle, S.; Williams, S. P.; Lowe, R. D.; Jayaraman, M. *J. Am. Chem. Soc.* **1993**, *115*, 4910. (f) Chen, T.-A.; Wu, X.; Rieke, R. D. *J. Am. Chem. Soc.* **1995**, *117*, 233.

(6) Elsenbaumer, R. L.; Jen, K.-Y.; Miller, G. G.; Eckhardt, H.; Shacklette, L. W.; Low, R. In *Electronic Properties of Conjugated Polymers*; Kuzmany, H., Mehring, M., Roth, S., Eds.; Springer Series in Solid State Sciences; Springer: New York, 1987; Vol. 76, p 400.

(7) Vidal, P. L.; Divisia-Blohorn, B.; Bidan, G.; Hazemann, J. L.; Kern, J. M.; Sauvage, J. P. *Chem. Eur. J.* **2000**, *6*, 1663.

(8) Vidal, P. L.; Divisia-Blohorn, B.; Bidan, G.; Sauvage, J. P.; Kern, J. M.; Hazemann, J. L. *Inorg. Chem.* **1999**, *38*, 4203.

(9) Divisia-Blohorn, B.; Genoud, F.; Borel, C.; Bidan, G.; Kern, J. M.; Sauvage, J. P. *J. Phys. Chem. B* **2003**, *107*, 5126.

(10) Guillerez, S.; Kalaji, M.; Lafolet, F.; Novaes Tito, D. *J. Electranal. Chem.* **2004**, *563*, 161.

(11) (a) Brédas, J. L.; Street, G. B. *Acc. Chem. Res.* **1985**, *18*, 309. (b) Heeger, A. J.; Kievelson, S.; Schrieffer, J. R.; Su, W.-P. *Rev. Mod. Phys.* **1988**, *781*, 60. (c) See for example: Genoud, F.; Kruszka, J.; Nechtschein, M.; Zagorska, M.; Kulszewicz-Bayer, I.; Pron, A. *J. Chim. Phys.* **1990**, *87*, 57.

(12) Magnuson, A.; Frapart, Y.; Abrahamsson, M.; Horner, O.; Akermark, B.; Sun, L.; Girerd, J. J.; Hammarström, L.; Styring, S. *J. Am. Chem. Soc.* **1999**, *121*, 89.

(13) Nechtschein, M. In *Handbook of Conducting Polymers*, 2nd ed.; Stoktheim, T. A., Elsenbaumer, R. L., Reynolds, J. R., Eds.; Marcel Dekker: New York, 1998; Chapter 5.

(14) (a) Chandrasekhar, P. *Conducting Polymers, Fundamentals and Applications, A Practical Approach*; Kluwer Academic Publishers: Norwell, MA, 1999; p 315. (b) Tormo, J.; Moreno, F. J.; Ruiz, J. Fajari, L.; Julia, L. *J. Org. Chem.* **1997**, *62*, 878.

(15) Tourillon, G.; Gourier, D.; Garnier, F.; Vivien, D. *J. Phys. Chem.* **1984**, *88*, 1049.

(16) Domalaga, W.; Lapkowski, M.; Guillerez, S.; Bidan, G. *Electrochim. Acta* **2003**, *48*, 2379.

(17) Panozzo, S.; Lafolet, F.; Trouillet, L.; Vial, J.-C.; Guillerez, S. *Synth. Met.* **2004**, *142*, 201.

(18) Wang, C.; Schindler, J. L.; Kannewurf, C. R.; Kanatzidis, M. G. *Chem. Mater.* **1995**, *7*, 58.

(19) (a) Cravino, A.; Neugebauer, H.; Luzzati, S.; Catellani, M.; Petr, A.; Dunsch, L.; Sariciftci, N. S. *J. Phys. Chem. B* **2002**, *106*, 3583. (b) Neugebauer, H.; Cravino, A.; Luzzati, S.; Catellani, M.; Petr, A.; Dunsch, L.; Sariciftci, N. S. *Synth. Met.* **2003**, *139*, 747.

(20) Yamamoto, T. *Bull. Chem. Soc. Jpn.* **1999**, *72*, 621.

(21) Yamamoto, T.; Maruyama, T.; Zhou, Z.; Ito, T.; Fukada, T.; Yoneda, Y.; Begum, F.; Ikeda, T.; Sasaki, S.; Takezoe, H.; Fukuda, A.; Kubota, K. *J. Am. Chem. Soc.* **1994**, *116*, 4832.

(22) (a) Motten, A. G.; Hanck, K.; DeArmond, M. K. *Chem. Phys. Lett.* **1981**, *79*, 541. (b) Gex, J. N.; DeArmond, M. K.; Hanck, K. *J. Phys. Chem.* **1987**, *91*, 1, 251.

(23) (a) Trznadel, M.; Zagorska, M.; Lapkowski, M.; Louarn, G.; Lefrant, S.; Pron, A. *J. Chem. Soc., Faraday Ttrans.* **1996**, *92*, 1387. (b) Zargoska, M.; Pron, A.; Lefrant, S. In *Handbook of Organic Conductive Molecules and Polymers*; Nalwa, H. S., Ed.; Wiley: Chichester, U.K., 1997; Vol. 3, Chapter 4.

(24) See for example: (a) Demanze, F.; Yassar, A.; Garnier, F. *Macromolecules* **1996**, *29*, 4267. (b) Jousselme, B.; Blanchard, P.; Oçafrain, M.; Allain, M.; Levillain, E.; Roncali, J. *J. Mater. Chem.* **2004**, *14*, 421. (c) Hotta, S. In *Handbook of Organic Conductive Molecules and Polymers*; Nalwa, H. S., Ed.; Wiley: Chichester, U.K., 1997; Vol. 2, Chapter 8.